A NEW METHOD FOR 2D-VECTOR BLOOD FLOW IMAGING BASED ON UNCONVENTIONAL BEAMFORMING TECHNIQUES

Matteo Lenge[1,2], Alessandro Ramalli[1], Andrea Cellai[1], Piero Tortoli[1], Christian Cachard[2], Hervé Liebgott[2]

[1] Information Engineering Dept., Università degli Studi di Firenze, Italy
[2]CREATIS, Université de Lyon ; CNRS UMR 5220 ; INSERM U1044 ; Université Lyon 1 ; INSA-Lyon, Villeurbanne, France

ABSTRACT

Conventional Ultrasound (US) Doppler methods for blood flow imaging are limited to velocity estimations only in the axial direction, i.e. along the beam direction. Transverse oscillations (TO) methods extend blood investigations towards multidimensional estimates, and detailed descriptions of complex and fast blood flows are achievable by high frame-rate (HFR) imaging methods. In this work, TO are coupled with plane-waves (PWs) to reconstruct radio-frequency (RF) images with bi-directional oscillations in the pulse-echo field. The achieved RF images are exploited by a 2D phase-based displacement estimator to produce 2D-vector flow maps. A preliminary simulation study confirmed the capability of the method to produce the designed oscillations in the RF pulse-echo fields as well as the possibility to obtain 2D-vector maps with errors lower than 10% in many different conditions.

Index Terms— Ultrasound, blood-flow imaging, high frame-rate imaging, plane waves, transverse oscillations

1. INTRODUCTION

The most important limitation of conventional US blood flow imaging is the estimation of only one component of the blood velocity vector (i.e. along the axial direction) [1]. To extend the estimation along multiple directions, the multi-beam approaches [2] combine several Doppler measurements ([3], [4]). Furthermore, the 2D cross-correlation function has been used to achieve bi-dimensional blood maps of the 2D-vector velocity, first by Trahey et al. (the "speckle-tracking" methods [5]), and, more recently, by Udesen et al. [6], exploiting the transmission of plane waves (PWs) at high frame-rate (HFR). Similar results are obtained in [7], where PWs imaging has been coupled with a frequency-domain algorithm. Another technique for blood flow imaging is the "transverse oscillations" (TO) theory [8], [9], which has been implemented in a real-time commercial system (BK Medical ApS, Denmark).

In this work, TO are coupled with PWs imaging to achieve 2D-vector maps of blood flow. The method implements an original parallel beamforming in reception, which consists in a dynamic apodization on the received signals to generate, in the pulse-echo field of the entire RF image, controlled oscillations in both the axial and the transverse direction. Such double oscillating images are exploited by a phase-based estimator, previously proposed for elastographic applications [10], to obtain the 2D-vector maps. In the following sections, the method is presented and tested by simulations in different conditions.

2. METHODS

2.1. Plane-waves transverse-oscillations imaging

64 elements of a linear array transducer are excited by sinusoidal bursts, to transmit plane-waves at 15 kHz pulse repetition frequency (PRF). The same elements are used to receive the echoes backscattered by the region of interest (ROI) under investigation. Each point of the i^{th} RF image (in the following, RF_i) is obtained by a conventional delay and sum beamforming [11]:

$$RF_i(z,x) = \sum_{j=1}^{64} w_j \, RF_s\left(\tau(\varepsilon_j, z, x)\right) \tag{1}$$

where j indicates one of the probe elements, ε_j is the transducer element position, (z,x) are the axial and lateral coordinates of the point, w_j is the receive apodization weighting function, RF_s is the received radio-frequency signals, and τ the travelling time from the point (z,x) to the transducer element (ε_j).

Transverse oscillations in the pulse-echo field are obtainable through a dynamic beamforming in receive [12]. Here, a double Gaussian for the receive apodization function w_j is employed:

This work has been supported by the European Fund for Regional Development for the 2007-2013 programming period (POR FES 2007-2013 CRO ASSO and MIMAUS Projects), by the Franco-Italian University (Galileo Project 2011-2012 n.26075WL) and CeLyA and PRIMES LabEx.

978-1-4799-2893-4/14/$31.00 ©2014 IEEE

$$w_j(\varepsilon_j, z, x) = \frac{1}{2}\left(e^{-\pi\left(\frac{\varepsilon_j - x - x_0}{\sigma_0}\right)^2} + e^{-\pi\left(\frac{\varepsilon_j - x + x_0}{\sigma_0}\right)^2}\right) \quad (2)$$

where x_0 is the position of the Gaussian peaks on the transducer, and σ_0 is their width at half maximum. Note that w_j depends on z because, according to the TO theory, x_0 has to be modulated as a function of depth (z) to obtain an oscillation with a constant transverse wavelength (λ_x):

$$x_0 = \frac{\lambda_z z}{\lambda_x} \quad (3)$$

where $\lambda_z = c/f_z$ is the axial oscillation, c the speed of sound and f_z the burst central frequency.

The apodization function is defined on a convenient subset of elements, and, as notable from (2), it is laterally centered on x. In general, if L is the width of each mainlobe of the Gaussian apodization, one axial line located at x is obtained by the beamforming of the *2L* channels selected in the neighborhood of x (i.e. L in each direction) (see Fig. 1). Since the RF dataset is the same for each line that has to be reconstructed, a parallel beamforming in receive is adoptable, to strictly reduce the algorithm execution time.

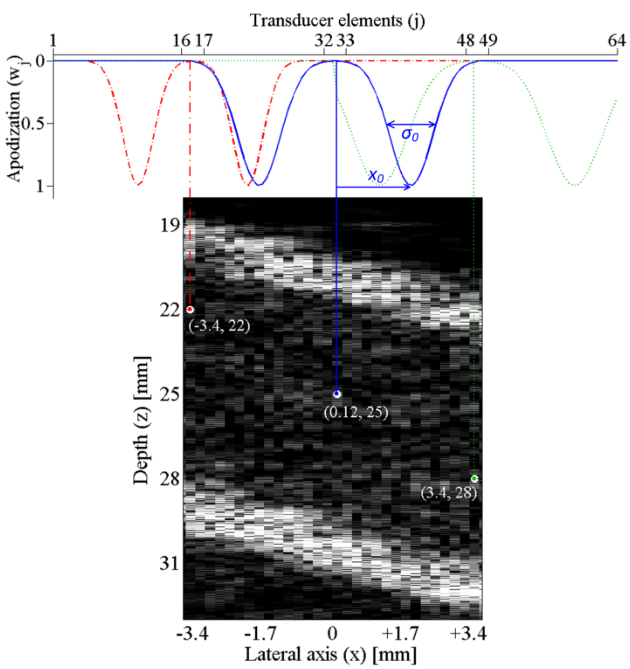

Fig. 1. The PWs-TO imaging method, with the apodization function on 64 RX channels and 16 elements for the Gaussian main-lobe (L), and a B-mode image of the simulated setup. As example, the point $(x, z) = (0.12, 25)$, located on the element $j = 33$, has been obtained beamforming the adjacent 32 RF channels (i.e. $j = \{17, 48\}$). The red dash-dotted lines correspond to the apodization function for the point $(x, z) = (-3.4, 22)$, and the green dotted lines correspond to the point $(x, z) = (3.4, 28)$.

2.2. 2D-vector phase-based estimator

The 2D-vector image is achieved by the phase-based estimator proposed by [10], that defines a mesh of blocks on the RF_i and locally calculates the 2D displacement (d_z,d_x) between two equivalent blocks that belong respectively to two consecutive RF_i:

$$d_z = \frac{\psi_1 + \psi_2}{4\pi f_z} \qquad d_x = \frac{\psi_1 - \psi_2}{4\pi f_x}$$

where ψ_1 and ψ_2 are the phase differences between the analytical images of the two RF_i, calculated respectively on the orthants 1 and 2. The velocity vector is obtained multiplying for the frame-rate (FR) the 2D displacements:

$$\vec{v} = (d_z\hat{z} + d_x\hat{x})\, FR = v_z\hat{z} + v_x\hat{x} \quad (4).$$

An extended vector map is obtained repeating the estimation on all the blocks defined into the ROI. Finally, velocities are filtered by a mean temporal filter on 20 frames.

2.3. Simulation setup

A Field II-based [13] [14] software has been used to simulate the scatterers movement inside a vessel phantom located at 25 mm depth, inclined of 70° with respect to the beam direction, with a 4 mm internal radius (see Fig. 1). The scatterers (25/mm^3 density) have been shaped to a parabolic steady flow with a 100 cm/s velocity peak, and the backscatter intensity was -20dB with respect to the walls.

The 64 elements of the linear probe (110% bandwidth @ 8 MHz, 245 µm pitch) have been excited by N_C sinusoidal cycles at f_z central frequency. Transverse oscillations at λ_x lateral wavelength have been generated apodizing the 64 RX channels with a double Gaussian function on 32 elements (L=16 elements for each mainlobe), and an RF_i extended on 32 lateral lines has been obtained.

The method performance at reference setup conditions (the bolded values in Tab. 1 represents "reference setup") has been compared with different conditions, obtained swapping each single parameter to different values.

A stationary echo-canceling filter has been used on 20 RF_i, to remove the backscattered contributions of the walls [6]. Setting the speed of sound (c) to 1480 cm/s and the system sampling frequency to 50 MHz, the spatial resolution δ_z was 14.8 µm in the axial direction, whereas in the lateral direction δ_x is 245 µm (i.e. the pitch). Finally, the phased-based algorithm has been employed adopting a block of (32x12) samples (axial and lateral size, respectively).

Tab. 1 – Simulation setup

PWs-TO parameters	*Value*
No. transmit cycles (N_C)	[3, **5**, 8, 11, 14]
Central frequency (f_z)	[5, **6**, 7, 8] MHz
Lateral wavelength (λ_x)	[0.49, 0.74, 0.98, 1.23, **1.47**, 1.72, 1.96] mm

Tab. 1. Simulation setup. The "reference setup" corresponds to the parameters in bold type. Note that the values for the lateral wavelengths correspond to [2, 3, 4, 5, **6**, 7, 8] lines.

2.4. Performance metrics

The method performance has been evaluated by the relative bias and the standard deviation of the estimated velocity ($\hat{v}$) compared to the theoretical parabolic profiles (v) calculated on 20 lines, uniformly distributed in the centre of the ROI. Metrics of each velocity component are defined as follows:

$$B_v = \frac{1}{N_l}\sum_{j=1}^{N_l}\frac{1}{v_0 N_d}\sum_{i=1}^{N_d}\frac{1}{N_f}\sum_{k=1}^{N_f}\left|\hat{v}(z_i, x_j, p_k) - v(z_i, x_j)\right|$$

$$\sigma_v = \frac{1}{N_l}\sum_{j=1}^{N_l}\frac{1}{{v_0}^2 N_d}\sum_{i=1}^{N_d}\frac{1}{N_f}\sum_{k=1}^{N_f}\left(\hat{v}(z_i, x_j, p_k) - v(z_i, x_j)\right)^2$$

where (z_i, x_j, p_k) indicates the point (z_i, x_j) of the frame p_k, v_0 is the component of the peak velocity, N_l is the number of estimation lines (20), N_d is the number of axial samples and N_f is the number of frames (499).

3. RESULTS

3.1. Pulse-echo field

The method capability to obtain double oscillating fields is demonstrated by Fig. 2, where a block of a simulated RF_i, obtained in the "reference setup" conditions (f_z = 6 MHz, λ_x = 1.47 mm), is considered.

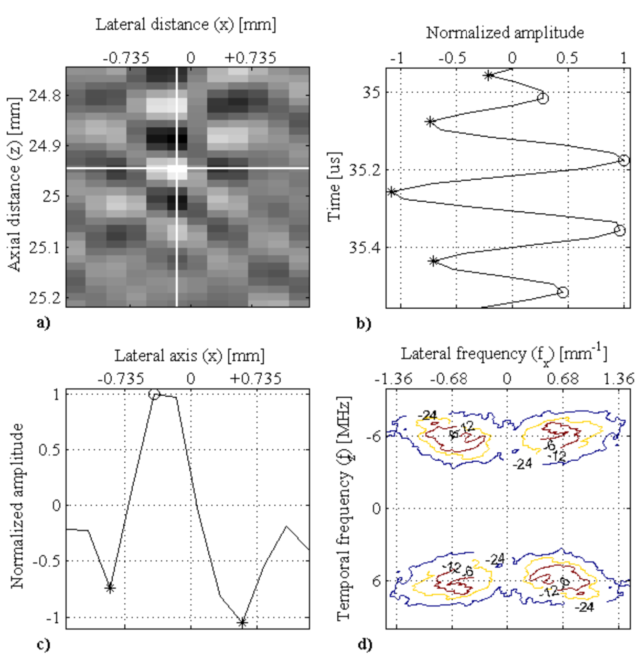

Fig. 2. The pulse-echo field of a block located at the center of a simulated vessel. In a) the double oscillating field. In b) the RF signal, and, in c), the TO signal are shown, both referred in a) to the vertical and the horizontal white sections, respectively. In d), the 2D-DFT of the block of a).

In particular, Fig. 2a shows the pulse-echo field of a single block located at the center of the vessel. The oscillations of an illustrative block along the axial and lateral directions are respectively illustrated in b) and c), and the 2D Discrete Fourier Transform (2D-DFT) of the block is shown in d). Pulse-echo field estimations on a block point out an axial oscillation f_z = 6.12 MHz, and the lateral oscillation (λ_x = 1.49 mm). The squared waveform is due to the poor lateral sampling frequency.

3.2. Blood flow simulations

The simulations were obtained changing the fundamental parameters of the PWs-TO method: the number of transmit cycles (Fig. 3a), the central frequency (Fig. 3b) and the lateral wavelength (Fig. 3c). The effects of the variation on the estimated velocity components (v_z, v_x) are evaluated in terms of the bias and the standard deviations defined in section 2.4.

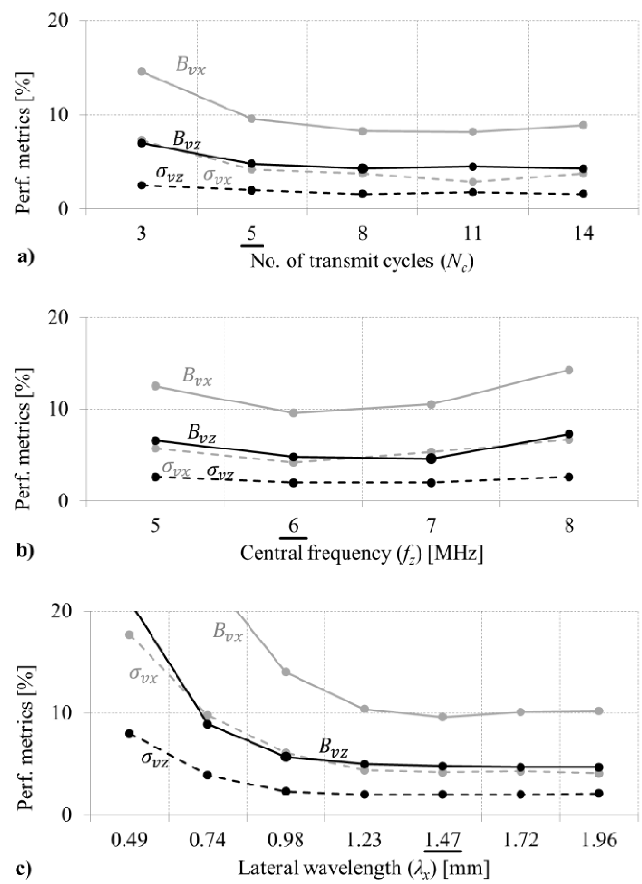

Fig. 3. Velocity performance metrics (bias and standard deviations) as functions of the varying parameters indicated in Tab. 1: in a) the number of transmit cycles (N_C), the central frequency in transmission (f_z), and the lateral wavelength (λ_x). Underlined values in the *x-axis* correspond to the "reference setup".

In Fig. 4, a vector map obtained by the method is illustrated. The gray-scaled B-mode image of the simulated vessel, obtained by the demodulation of the RF_i, is overlaid by the vector map that describes the parabolic blood flow.

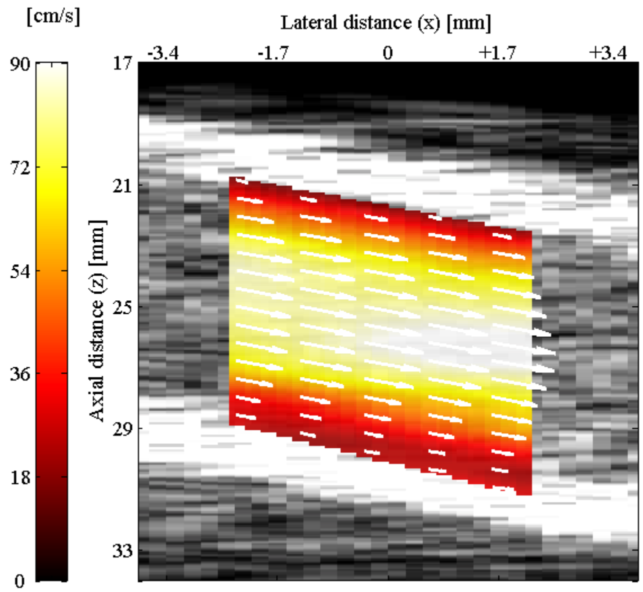

Fig. 4. A vector map of the simulation at the reference setup. The number of the arrows is undersampled by a factor of 50 with respect to estimations, in order to facilitate the comprehension by the reader.

Method performance is described also by the histograms of Fig. 5, which illustrates the distributions of the velocity components obtained in a single block located at the center of the vessel. The mean values of each distribution result in the components of the velocity vector centered into the block.

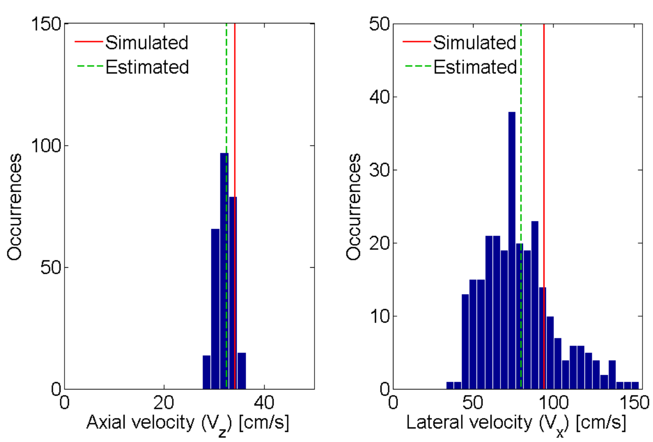

Fig. 5. Histograms of the distribution of the axial (a) and the lateral (b) velocities inside a block located at the geometrical center of the vessel (the same of Fig. 2). Red line indicates the simulated velocity, while the dashed green line indicates the estimated velocities (i.e. the mean value of the distribution).

4. DISCUSSION AND CONCLUSION

In this paper, a new method for US imaging, based on the PWs transmission and the TO theory, is presented. The method has been coupled with a phase-based estimator to achieve 2D vector maps of simulated blood flows.

The method performance is described with simulations obtained changing specific parameters of the US system. The pulse-echo field in Fig. 2 Fig. 4shows that the here proposed PWs-TO beamforming is capable to generates images with the expected oscillations in the pulse-echo field. The quality of such images is adequate for the phase-based estimator, achieving extended 2D-vector maps of the blood velocity (Fig. 4) with performance metrics around 10%. In particular, if the number of burst cycles (N_C) is increased (Fig. 3a), the power in transmission is higher, and better performance is obtained. Increasing N_C is commonly adopted in TO imaging based on the receive beamforming (e.g. the double Gaussian apodization) [15], in order to compensate the attenuation of RF signals, that is unavoidable to obtain the oscillations in the transversal direction.

Results of Fig. 3b corresponds to the TO theory, that suggests the use of lower central frequencies to obtain better transverse oscillations (and performance), although it is important to remain in the full-band of the transducer.

Fig. 3c outlines the drop of performance with lower λ_x. Such errors are unrelated with the aliasing, which commonly affects the displacement estimators which are based on the calculation of the phase difference of complex signals. Using a so high frame-rate, the lateral peak velocities (93cm/s at 70° of beam-to-flow angle) corresponds to a lateral displacement (0.03 mm at 15kHz frame-rate) in the order of $\lambda_x/20$, which is much lower than the theoretical aliasing limit ($\lambda_x/2$). Results of Fig. 3c highlight that if λ_x is lower than 5 times the pitch (1.23 mm), the performance drops because the phase of transverse oscillation is quantized with a number of points that is insufficient for the estimator, and, according to the theory, fast TO oscillations cannot be obtained for extended depths.

Future work will be done to illustrate the method capability to obtain the designed double-oscillations fields, with point spread functions and statistical indexes (bias and standard deviation), that aimed to describe quantitatively the oscillations obtained with different system parameters. Results will also guide the optimization of the displacement estimator, and different block sizes in the axial and the lateral directions will be tested. The performance in terms of the computational load will be estimated and compared to other methods implementations. To evaluate the method sensitivity to different conditions, blood flow simulations will be performed changing the beam-to-flow angle, the barycenter depth and the velocity profile of the vessel. In-vitro and in-vivo experiments will be made, to test method performance in operative conditions.

REFERENCES

[1] D. H. Evans and W. N. McDicken, *Doppler Ultrasound: Physics, instrumentation and signal processing*, 2nd edition. Chichester: Wiley, 2000.

[2] B. Dunmire, K. W. Beach, K.-H. Labs, M. Plett, and D. E. Strandness Jr., "Cross-beam vector Doppler ultrasound for angle-independent velocity measurements," *Ultrasound in Medicine & Biology*, vol. 26, no. 8, pp. 1213–1235, Oct. 2000.

[3] M. D. Fox, "Multiple crossed-beam ultrasound Doppler velocimetry," *IEEE Transactions on Sonics and Ultrasonics*, vol. 25, no. 5, pp. 281 –286, Sep. 1978.

[4] O. Bonnefous, "Measurement of the complete (3D) velocity vector of blood flows," in *1988 IEE Ultrasonics Symposium (IUS)*, 1988, vol. 2, pp. 795 – 799.

[5] G. E. Trahey, J. W. Allison, and O. T. Von Ramm, "Angle Independent Ultrasonic Detection of Blood Flow," *IEEE Transactions on Biomedical Engineering*, vol. BME-34, no. 12, pp. 965–967, Dec. 1987.

[6] J. Udesen, F. Gran, K. Hansen, J. A. Jensen, C. Thomsen, and M. B. Nielsen, "High frame-rate blood vector velocity imaging using plane waves: Simulations and preliminary experiments," *IEEE Transactions on Ultrasonics, Ferroelectrics and Frequency Control*, vol. 55, no. 8, pp. 1729 –1743, Aug. 2008.

[7] M. Lenge, A. Ramalli, E. Boni, A. Cellai, H. Liebgott, C. Cachard, and P. Tortoli, "Frequency-domain high frame-rate 2D vector flow imaging," in *Ultrasonics Symposium (IUS), 2013 IEEE International*, 2013, pp. 643–646.

[8] J. A. Jensen and P. Munk, "A new method for estimation of velocity vectors," *IEEE Transactions on Ultrasonics, Ferroelectrics and Frequency Control*, vol. 45, no. 3, pp. 837 –851, May 1998.

[9] M. J. Pihl and J. A. Jensen, "Measuring 3D Velocity Vectors using the Transverse Oscillation Method," in *2012 IEEE Ultrasonics Symposium (IUS)*, 2012, pp. 1881–1885.

[10] A. Basarab, P. Gueth, H. Liebgott, and P. Delachartre, "Phase-based block matching applied to motion estimation with unconventional beamforming strategies," *IEEE Transactions on Ultrasonics, Ferroelectrics and Frequency Control*, vol. 56, no. 5, pp. 945 –957, May 2009.

[11] G. Montaldo, M. Tanter, J. Bercoff, N. Benech, and M. Fink, "Coherent plane-wave compounding for very high frame rate ultrasonography and transient elastography," *IEEE Transactions on Ultrasonics, Ferroelectrics and Frequency Control*, vol. 56, no. 3, pp. 489 –506, Mar. 2009.

[12] H. Liebgott, A. Basarab, P. Gueth, D. Friboulet, and P. Delachartre, "Transverse oscillations for tissue motion estimation," *Ultrasonics*, vol. 50, no. 6, pp. 548–555, May 2010.

[13] J. A. Jensen, "FIELD: A Program for Simulating Ultrasound Systems," in *10th Nordicbaltic Conference On Biomedical Imaging*, 1996, vol. 4, sup. 1, pp. 351–353.

[14] J. A. Jensen and N. B. Svendsen, "Calculation of pressure fields from arbitrarily shaped, apodized, and excited ultrasound transducers," *IEEE Transactions on Ultrasonics, Ferroelectrics and Frequency Control*, vol. 39, no. 2, pp. 262–267, Mar. 1992.

[15] J. Udesen and J. A. Jensen, "Investigation of transverse oscillation method," *IEEE Transactions on Ultrasonics, Ferroelectrics and Frequency Control*, vol. 53, no. 5, pp. 959–971, May 2006.